PROCEEDINGS OF SCIENCE

Polarimetry measurements of surfacic strong magnetic field produced by high power laser

Pierre Forestier-Colleoni*, **Dimitri Batani, Frédéric Burgy, Fanny Froustey, Sébastien Hulin, Emmanuel d'Humières, Katarzyna Jakubowska, Laurent Merzeau, Konstantin Mishchik and João Jorge Santos**
CELIA, Université de Bordeaux, Talence, France
E-mail: forestier@celia.u-bordeaux1.fr

Daniel Papp
ELI-HU, Szeged, Hungary

Christopher Spindloe
Rutherford Appleton Laboratory, Didcot, United Kingdom

The experimental investigation of intense laser-solid interaction, with particular attention to the mechanisms of fast electron beam (FEB) generation and propagation, is of paramount importance for the development of applications based on FEB-energy transport into target depth, such as fast ignition of inertial confined targets, laser-acceleration of ion beams, or isochoric creation of warm dense matter states. In particular, the characterization of the structure of the magnetic fields developing at the interaction surface would allow to understand FEB parameters at the source, such as its energy, radius and angle distributions. The goal here is to characterize experimentally the spatial and temporal evolution of this magnetic field in a "pump-probe" experiment (with pump laser at ω, 45° incidence and probe at 2ω, normal incidence) with a space-resolved polarimetry diagnostic. During propagation inside the magnetized plasma created by the pump beam, the polarization of the probe changes due to the Cotton-Mouton and Faraday effects. We obtained, at different times, 2D maps of the probe polarization variations (and hence of the magnetic fields) over a region much larger that the focal spot of the main beam. The analysis of the results shows in particular, 1 ps after the interaction of the pump beam with the target surface, an average magnetic field amplitude of the order of some MGauss distributed over a region $\approx 50\mu$m in diameter centered around the interaction spot of the pump laser.

First EPS Conference on Plasma Diagnostics - 1st ECPD,
14-17 April 2015
Villa Mondragone, Frascati (Rome) Italy

*Speaker.

PoS(ECPD2015)044

1. Introduction

The physics of laser-solid interactions and in particular the generation of a Fast Electron Beam (FEB), created by the interaction of a high intensity laser focused onto the surface of a solid target, can be very important for various applications such as fast ignition laser driven fusion[1][2], creation of ion or electron beams[3], Warm dense matter studies [4][5][6],etc. Yet, many fondamental aspects of FEB generation remain obscure. Its initial divergence, for example, remain to be fully understood. This divergence could be due to strong magnetic fields at the surface of the target (near critical density n_c)[7]. The diverging magnetic structure could be created by the Weibel instability due to two electron beams (the FEB and the neutralizing return current of background electrons). Experimental data concerning this magnetic field is insufficient and its characterization was the goal of our experiment. We used a pump-probe polarimetry method to investigate the Cotton-Mouton effects and estimate the $\vec{B}$-spatial distribution as a fucntion of time. The principal idea is to make the probe beam propagate through the magnetized plasma. This magnetized plasma change the polarization of the laser beam. An optical, spatial-resolved polarimeter was developed to characterize the polarization of the reflected beam, and from there, describe the structure of the B-field at the target surface. Our work stands out from previous woks of surface magnetic field characterization by polarimetric measurements of probe reflected laser light[8][9] by providing a simultaneous space and time information, over a field of view greater than the magnetized region. This allows to clearly highlight the extent and structure of the magnetic field.

2. Experiment

In this experiment we used the laser facility ECLIPSE at the CELIA Laboratory, Université de Bordeaux. This laser is a Ti-Sa (wavelength $\lambda = 800$ nm). Its main beam (pump) delivers an energy up to 100mJ on target for a duration of 27 fs (FWHM, supposing a Gaussian) with an 10^{-5} power contrast. It is focused by an off-axis parabola to a focal spot of 8μm (FWHM), with an angle of 45° with respect to the target normal (p-polarization), yielding a maximum intensity on target of $\approx 10^{18}$W/cm^2. There are two probe beams with ≈ 5 mJ each. One of the beams is doubled in frequency (using a Beta-Barium Borate (BBO) crystal) and focused on target using a 220 mm focal length lens at normal incidence to obtain a focal spot on target about 200μm. A delay line provided the time delay Δt of the probing over the range of -2 ps to 6 ps and a resolution of 30 fs with respect to the pump beam. This beam was reflected at the cut-off density ($\omega_{pe}/\omega_{probe} + \omega_{ce}/\omega_{probe} = 1$ with $\omega_{pe} = \sqrt{4\pi n_e e^2/m_e}$ the electron plasma pulsation and $\omega_{ce} = eB/cm_e$ the electron cyclotron pulsation). This cut-off density is generally deeper in the target than the critical density for the pump beam ($n_{c\ probe} = 4n_{c\ pump}$), density of fast electron generation. The reflected probe beam is collected into a polarimeter/imaging system of magnification 10 and resolution $\approx 12\mu$m. The second probe beam was used for side on interferometry measurement of the plasma density. The used target is a 1μm coating of Al on a 1mm thick SiO_2 glass of optical quality $\lambda/5$. Figures 1a and 1b show the setup of the experiment.

The used polarimeter is a home-made device that creates four reflectivity images of the target corresponding to the four Stokes parameters [10][11] of the probe beam, related to different polarization information (see below). This device included two CCD (12 bits), each one capturing two

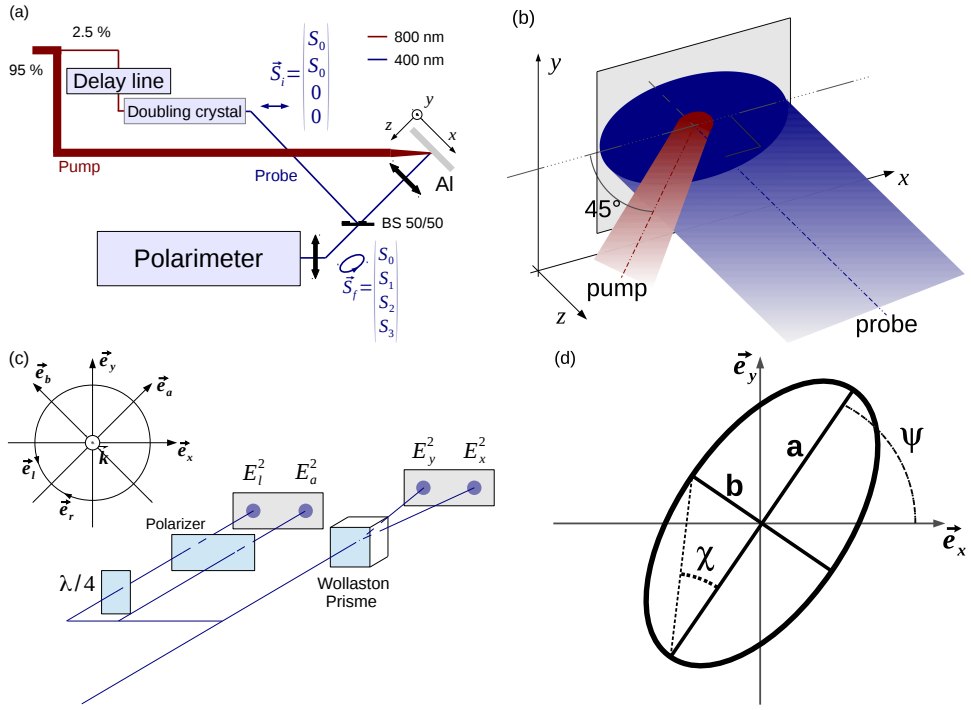

Figure 1: (a,b and c) Experimental setup of the experiment and (d) definition of the probe laser polarization parametres.

of those images. On the first camera we measured the intensity of the probe beam on two orthogonal directions, named E_x^2 and E_y^2 (direction $\vec{e}_x$ and $\vec{e}_y$). Those two components were obtained by using a Wollaston prism, spliting the two projections of the electric field by a 2° angle. The second camera is used to obtain the projection of the electric field of the probe beam on a direction called $\vec{e}_a$, at 45° from $\vec{e}_x$. This gives the projection E_a^2. On the same CCD, we obtained the projection E_l^2 (direction $\vec{e}_l$), representing the circular polarization of the light. These projections were obtained by a linear polarizer at 45° (for E_a^2) and a polarizer at 45° in combinatison with a $\lambda/4$ wave-plate at 0° (for E_l^2). This is represented in the Figure 1c. These four projections allow us to measure the Stokes parameters and so infer the complete polarization of the reflected probe light. To do that, we used the definition of the Stokes parameters

$$\vec{S} = \begin{pmatrix} S_0 \\ S_1 \\ S_2 \\ S_3 \end{pmatrix} = \begin{pmatrix} E_x^2 + E_y^2 \\ E_x^2 - E_y^2 \\ E_a^2 - E_b^2 \\ E_r^2 - E_l^2 \end{pmatrix} = \begin{pmatrix} E_x^2 + E_y^2 \\ E_x^2 - E_y^2 \\ 2E_a^2 - S_0 \\ S_0 - 2E_l^2 \end{pmatrix} \tag{2.1}$$

and the fact that on each orthogonal base the intensity S_0 of the beam is equal (this means $S_0 = E_x^2 + E_y^2 = E_a^2 + E_b^2 = E_r^2 + E_l^2$). For an easier visualization of the different changes of polarization, we can define two angles, χ and ψ, representing respectively the ellipticity of the polarization and

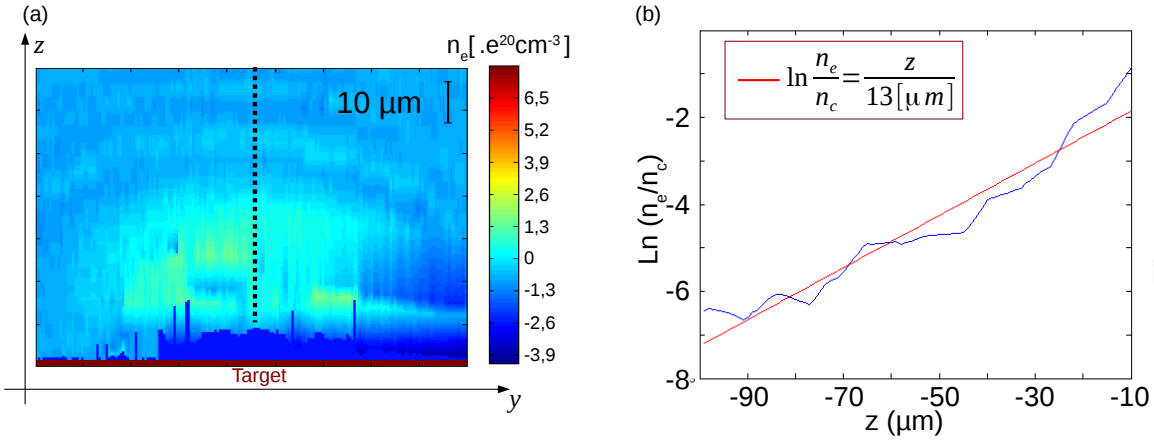

Figure 2: (a) Density map obtained by interferometry at grazing incidence to the target surface at $\Delta t = 0$ and (b) logarithm of the density profile as a function of z (line-out from (a) indicated by the dashed line)with a fit to obtain the gradient length.

the main axis orientation of the polarization (Figure 1d):

$$\chi = \frac{1}{2}\sin^{-1}\left(\frac{S_3}{S_0}\right) \tag{2.2}$$

$$\psi = \frac{1}{2}\tan^{-1}\left(\frac{S_2}{S_1}\right) \tag{2.3}$$

These angles are particulary useful because the different effects of the magnetic field on the polarization of the laser beam can be directly related to those angles. The first of these effects is the Faraday rotation which directly changes ψ if the magnetic field is parallel to the direction of propagation of the light $\vec{k}$. For a simple case

$$\delta\psi = \frac{1}{2}\int XY_{\parallel}\frac{\omega}{c}dz \tag{2.4}$$

with $X = n_e/n_c$, $Y = \omega_{ce}/\omega$, $Y_{\parallel} = Y\cos\theta$, θ the angle between the ambient magnetic field with the direction of propagation of the light $\vec{k}$ and ω the laser pulsation. For this equation we suppose $X << 1$ and $Y << 1$. The second is the Cotton-Mouton effect, changing the ellipticity of the polarization (directly χ) if the magnetic field is perpendicular to $\vec{k}$. For a simple case

$$\tan\chi = \frac{b}{a} = \frac{1}{2}\int XY_{\perp}^2\sin 2\beta\frac{\omega}{c}dz \tag{2.5}$$

with β the complementary angle between the direction of the ambient magnetic field and the principal axes of polarization of the light, $X << 1$, $Y << 1$ and $Y_{\perp} = Y\sin\theta$. For both effects, it is important to know the density of the probed plasma. An interferometry at grazing incidence allowed to estimate an electron density with a typical gradient length of $\approx 13\mu$m at $\Delta t = 0$ (Figure 2).

With this formalism we can obtain the change of polarization of the probe beam (initially $S_{probe} = (1,1,0,0)$ corresponding to a linear polarisation) created by the magnetic field of the plasma.

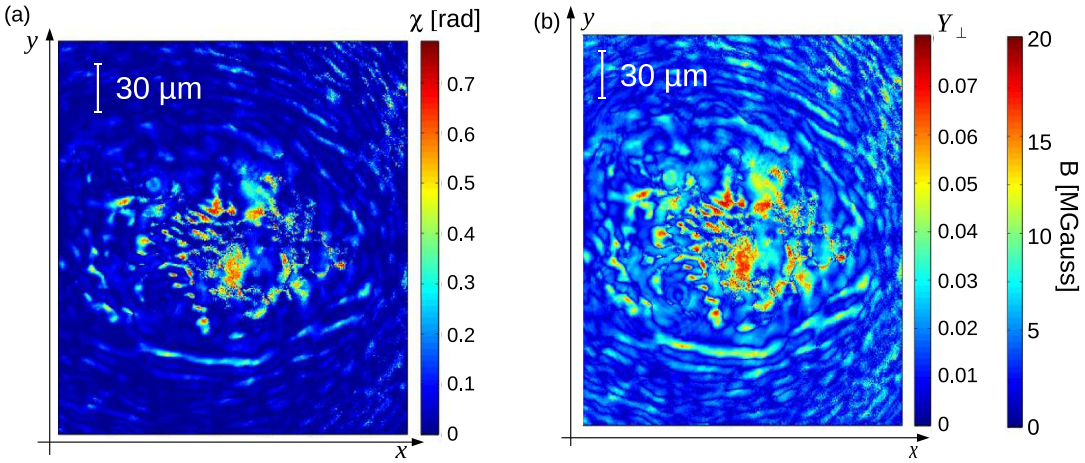

Figure 3: (a) Surfacic distribution of the angle χ of the probe beam and (b) $Y_\perp = (\omega_{ce}/\omega)\cos\theta$ and corresponding $B_\perp$ obtained using the equation 2.5 for a density gradient of 13μm, 1 ps after the interaction of the pump beam, for an intensity of 2.1×10^{17} W/cm^2

3. Preliminary results

A result example of the 2D map of the angle χ (obtained for an intensity on target of $\approx 2\times10^{17}$ W/cm^2) is shown in Figure 3a. From this result, we can estimate the spatial distribution of the B-field over the target surface (averaged over the penetration lenght of the probe laser) by simply using equation 2.5. We supposed that X and $Y << 1$, and in order to have a simple idea of the magnetic field for each position (x,y), we supposed a constant magnetic field during the laser propagation ($\partial Y_\perp/\partial z = 0$). This gives, from equation 2.5, $Y_\perp^2 = 2cb/(a\omega\int X\sin 2\beta dz)$. The Result is plotted in Figure 3b showing a map of the perpendicular magnetic field $Y_\perp$ the magnetic field, with values up to ≈ 20 Mgauss, is bistributed over a region of approximately 50 $\times$ 50 μm up to 20 MGauss. Strong inhomogeneities are present on this figure and can be due to magnetic or density fluctuations near the critical density. We are still carrying out a correlation with fluctuations on these two quantities from PIC simulations and from interferometry measurements (for the density).

In our experiment we made scans in delay and pump-laser energy. The obtained results are summarized in Figures 4a and 4b. The average perpendicular magnetic field decreases by a factor 2 from a maximum of ≈ 17 MGauss at $\Delta t \approx 0.3$ ps over a characteristic time of $\approx 2.6\pm0.5$ ps. A ≈ 7 MGauss field is likelly to subsist for later times, following the hydrodynamic plasma expansion. It's also possible to observe before the interaction of the pump laser with the target (Δt <0) a small average magnetic field of ≈ 250 kGauss. This magnetic field is undoubtedly an effect of the laser ASE-pedestal as its value is well above the detection threshold of ≈ 100 kGauss estimated from probe only reference acquisitions. It is difficult to drive a clear conclusion from the dependence of the magnetic field strength on the laser intensity (Figure 3b) because of the scarse number of data points. Yet, there is no significant variation on the results for the range of $2-10\times10^{17}$W/cm^2. Still, a lot of work remains to do, as defining better the change of polarization due to magnetic fields (analytic work) and benchmark our results with PIC simulations (in process).

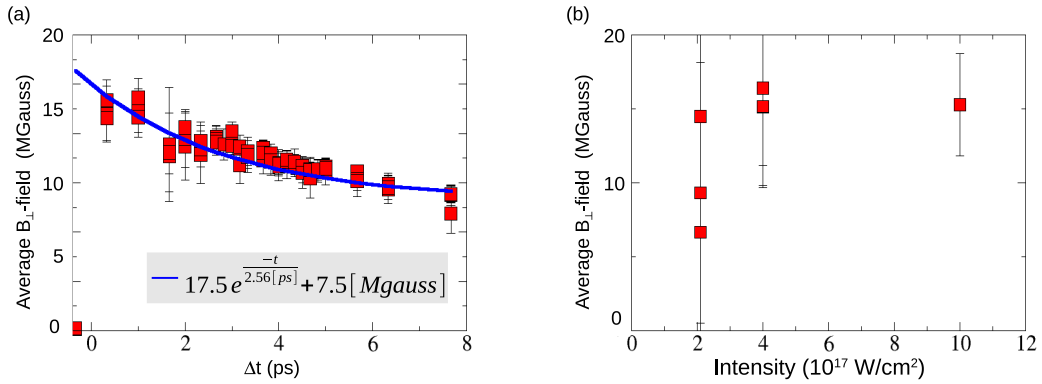

Figure 4: (a) Average perpendicular magnetic field $< B_\perp >$ as a fonction of time for 2.1×10^{17} W/cm^2 laser intensity and (b) function of the laser intensity at $\Delta t = 1$ ps.

References

[1] M. Tabak et al ., *Ignition and high gain with ultrapowerful lasers*, *Phys. Plasmas* **1** (1626) 1994.

[2] P. Norreys et al ., *Fast electron energy transport in solid density and compressed plasma*, *Nucl. Fusion* **54** (054004) 2014.

[3] K.W.D. Ledingham and W. Galster, *Laser-driven particle and photon beams and some applications*, *New. J. Phys.* **12** (045005) 2010.

[4] A. Saemann et al ., *Isochoric Heating of Solid Aluminum by Ultrashort Laser Pulses Focused on a Tamped Target*, *Phys. Rev. Lett.* **82** (4843) 1999.

[5] F. Perez et al ., *Enhanced Isochoric Heating from Fast Electrons Produced by High-Contrast, Relativistic-Intensity Laser Pulses*, *Phys. Rev. Lett.* **104** (085001) 2010.

[6] D.J. Hoarty et al ., *Observations of the Effect of Ionization-Potential Depression in Hot Dense Plasma*, *Phys. Rev. Lett.* **110** (265003) 2013.

[7] J.C. Adam, A.Héron and G. Laval, *Dispersion and Transport of Energetic Particules due to the Interaction of Intense Laser Pulses with Overdense Plasmas*, *Physical review letters* **97** (205006) 2006

[8] K. Subhendu, S. Mondal, G. Ravindra Kumar, S. Sengupta, A. Das and P.K. Kaw, *Polarimetric detection of laser induced ultrashort magnetic pulses in overdense plasma*, *Physics of plasmas* **16** (043114) 2009.

[9] S. Mondal et al., *Measurement of hot electron transport in overdense plasma VIA self induced giant magnetic pulses* , *J. Phys.: Conf. Ser.* **244** (022049) 2010.

[10] S.E. Segre, *A review of plasma polarimetry - theory and methods*, *Plasma Physics and Controlled Fusion* **41** (2-R57) 1999.

[11] McMaster, William H., *Polarization and the Stokes Parameters*, *American Journal of Physics* **22** (6,351-362) 1954.